

## Emergence of order in textured patterns

Gemunu H. Gunaratne,<sup>1,2</sup> Anuradha Ratnaweera,<sup>2</sup> and K. Tennekone<sup>2</sup>

<sup>1</sup>*Department of Physics, The University of Houston, Houston, Texas 77204*

<sup>2</sup>*The Institute of Fundamental Studies, Kandy, Sri Lanka*

(Received 28 August 1998)

A characterization of textured patterns, referred to as the disorder function  $\bar{\delta}(\beta)$ , is used to study properties of patterns generated in the Swift-Hohenberg equation (SHE). It is shown to be an intensive, configuration-independent measure. The evolution of random initial states under the SHE exhibits two stages of relaxation. The initial phase, where local striped domains emerge from a noisy background, is quantified by a power-law decay  $\bar{\delta}(\beta) \sim t^{-(1/2)\beta}$ . Beyond a sharp transition, a slower power-law decay of  $\bar{\delta}(\beta)$ , which corresponds to the coarsening of striped domains, is observed. The transition between the phases advances as the system is driven further from the onset of patterns, and suitable scaling of time and  $\bar{\delta}(\beta)$  leads to the collapse of distinct curves. The decay of  $\bar{\delta}(\beta)$  during the initial phase remains unchanged when nonvariational terms are added to the underlying equations, suggesting the possibility of observing it in experimental systems. In contrast, the rate of relaxation during domain coarsening increases with the coefficient of the nonvariational term. [S1063-651X(99)09405-2]

PACS number(s): 05.70.Ln, 82.40.Ck, 47.54.+r

### I. INTRODUCTION

The study of spatio-temporal patterns has received considerable impetus from a series of elegant experiments and theoretical developments based on symmetry considerations. Recent experimental studies include those on reaction diffusion chemical systems [1], convection in fluids [2] and gases [3], ferrofluids [4], and vibrated layers of granular material [5]. These results have been supplemented with patterns generated in (relatively) simple model systems [6–8]. The most complete theoretical treatments of patterns rely on the study of symmetries of the underlying system and those of the patterns [9]. Unfortunately, this analysis is restricted to periodic or quasiperiodic patterns. A theoretical analysis of more complex states requires the identification of suitable “variables” to describe a given pattern. Examples of such variables include the structure factor [10], the correlation length [11–13], and the density of topological defects [14]. In this paper we study properties of another characterization, referred to as the “disorder function” [15,16].

The patterns studied are generated in physical systems (and models) whose control parameters are uniform in space and time; thus, they result from spontaneous symmetry breaking. The simplest class of nontrivial structures is periodic. They are typically striped, square, triangular, or hexagonal patterns that form in perfect, extended arrays [6]. To obtain periodic patterns, the initial state of the system and/or the boundary conditions need to be carefully prepared. A second class consists of periodic patterns whose “unit cells” have additional structure [17,18]. A field describing periodic arrays can be expanded in a few plane waves.

The patterns described above contain a unit cell that is repeated on a “Bravais lattice” to generate a plane-filling structure. The qualitative description of the pattern involves the characterization (in terms of symmetries) of the unit cell and the generators of the Bravais lattice. For example, the unit cell of a honeycomb lattice is  $D_6$ -symmetric, and the

Bravais lattice is generated by two unit vectors  $120^\circ$  apart.

Quasiperiodic patterns have also been observed under suitable experimental conditions [19]. Their symmetries can be observed in Fourier space. For example, the spectrum of a quasicrystal is tenfold symmetric [20]. Quasiperiodic patterns can be described using a few “principal” plane waves along with their nonlinear couplings.

The bifurcations to and from a given periodic (or quasiperiodic) state can be studied using the “Landau equations,” which once again rely on the symmetries of the physical system and the pattern [21]. The information used is that, since the pattern is generated by symmetry breaking, a second pattern obtained under the action of any symmetry of the *physical system* has identical features. The imposition of this equivalence (supplemented by the elimination of “higher-order” terms) gives the normal form equations of the pattern. They contain information on aspects of dynamics of the pattern and details about its bifurcations [9].

Patterns such as those of Figs. 1 and 2 (which are generated in a model system) do not belong to the classes discussed above. These structures, referred to as “textured” or “natural” patterns [22], are observed when the initial states from which they evolve are not controlled. Similar structures are seen in small aspect ratio systems when the boundaries play a significant role in the creation of the pattern [6].

There is no (nontrivial) global symmetry of textures; consequently, they cannot be characterized using symmetry groups. Note also that a second realization of the experiment (e.g., starting from a different set of initial conditions) will give a pattern that is vastly different in detail [such as Figs. 1(a) and 1(b)]. In spite of these differences, one can clearly recognize similarities between distinct patterns. For example, the correlation length and the density of topological defects of the two textures shown in Fig. 1 are similar. In contrast, patterns generated under other external conditions (e.g., Fig. 2) have different characteristics. A theoretical treatment of textured patterns requires a “configuration independent” description.

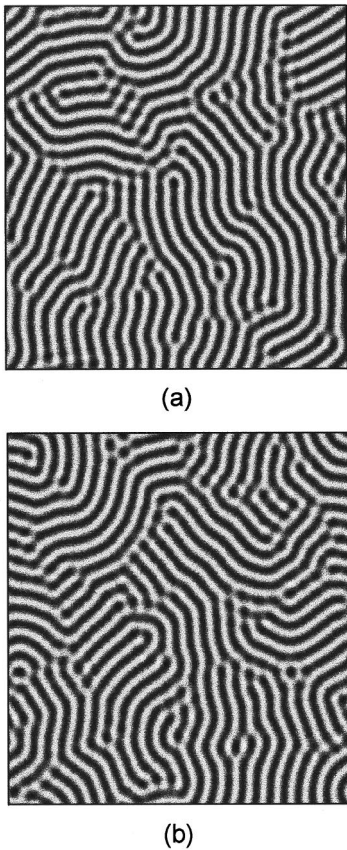


FIG. 1. Two patterns generated by evolving random initial states via the Swift-Hohenberg equation for 1600 time units. The parameters used were  $D=0.1$ ,  $\epsilon=0.2$ ,  $\nu=2$ , and  $k_0=1$ . The initial states consisted of white noise whose intensity varied between 0 and  $10^{-3}$ . Periodic boundary conditions were imposed on the square domain of  $256 \times 256$  lattice points, the length of whose sides are  $(48\pi/k_0)$ .

In Sec. II, we introduce the disorder function  $\bar{\delta}(\beta)$  whose definition was motivated in part by the argument leading to the derivation of Landau equations; for patterns generated in uniform, extended systems,  $\bar{\delta}(\beta)$  is required to be invariant under rigid motions of a labyrinthine pattern [15,16]. The main results of the paper, which include properties of the disorder function and its application to provide a quantitative description of the relaxation of the patterns from an initially random state, are presented in Secs. III and IV. The underlying spatio-temporal dynamics is given by the Swift-Hohenberg equation (SHE) and one of its variants. We first provide evidence to support the claim that the disorder function consists of intensive, configuration-independent variables. The use of  $\bar{\delta}(\beta)$  shows that pattern relaxation occurs in two distinct stages separated by a sharp transition. We also study changes in the relaxation profile when the system is driven further away from the onset of patterns. In Sec. IV, we discuss the effects of adding nonvariational terms to the SHE.

## II. THE DISORDER FUNCTION

Textured patterns observed in experimental systems [1–5] and those shown in Figs. 1 and 2 can be described by a scalar

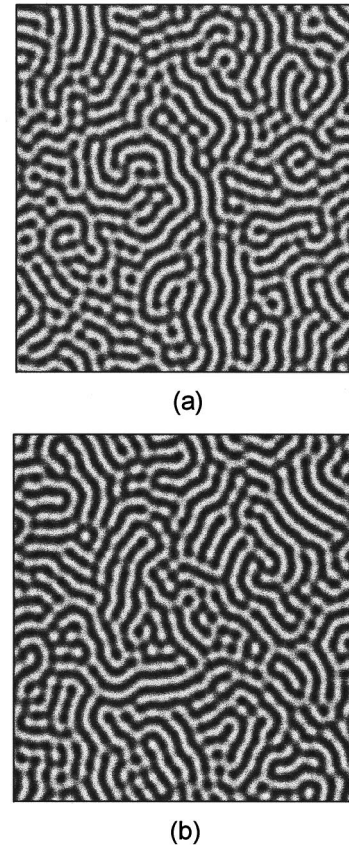


FIG. 2. Two patterns generated by evolving a random initial state via the Swift-Hohenberg equation for 2400 time units. The parameters used for the integration were  $D=0.01$ ,  $\epsilon=0.4$ ,  $\nu=2$ , and  $k_0=1/3$ . The initial states consisted of white noise whose intensity varied between  $\pm 10^{-2}$ . The length of each side of the square is  $(48\pi/k_0)$ .

field  $v(\mathbf{x})$  which is smooth, except perhaps at the defect cores. However, unless the patterns are trivial (e.g., perfect stripes, target patterns) the analytical form of the field is unknown. Consequently, it is difficult to determine a set of “configuration-independent” characteristics of structures generated under similar conditions. We impose instead a weaker requirement, that the characterizations remain invariant under the action of the symmetries of the underlying physical system; i.e., translations, rotations, and reflections [15].

Labyrinthine patterns are locally striped; in a suitable neighborhood  $v(\mathbf{x}) \sim \sin(\mathbf{k} \cdot \mathbf{x})$ , where the modulus  $k_0$  ( $\equiv |\mathbf{k}|$ ) of the wave vector does not vary significantly over the pattern. Structures generated in experiments and model systems include higher harmonics due to the presence of nonlinearities in the underlying system; they only contribute to the shape of the cross section of stripes. In order to use the simplest characterization of textures, we eliminate these harmonics by the use of a suitable window function in Fourier space. For experimental patterns (which do not have periodic boundary conditions) this is a nontrivial task, and a method to implement it is described in Ref. [24].

These considerations lead to the definition of a family of measures, referred to as the disorder function [16],

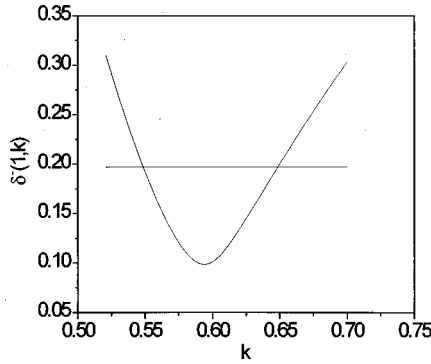


FIG. 3. The behavior of  $\bar{\delta}(1)$  as a function of the wave number  $k$  (in arbitrary units) for a labyrinthine pattern.  $k_0$  is estimated to be the (unique) minimum of the curve. The width  $\Delta k$  is defined to be the distance between the  $k$  values at which  $\bar{\delta}(1)$  reaches twice its minimum.

$$\delta(\beta) = (2 - \beta) \frac{\int da |(\Delta + k_0^2)v(\mathbf{x})|^\beta}{k_0^{2\beta} \langle |v(\mathbf{x})| \rangle^\beta}, \quad (1)$$

where  $\langle |v(\mathbf{x})| \rangle$  denotes the mean of  $|v(\mathbf{x})|$ , and  $\delta(\beta)$  has been normalized so that the “intensive variables”  $\bar{\delta}(\beta) = \delta(\beta)/\int da$  are scale invariant. The moment  $\beta$  lies between 0 and 2. Local deviations of the patterns from stripes (due to curvature of the contour lines [15]) contribute to  $\delta(\beta)$  through the Laplacian, while variations of the width of the stripes contribute via the choice of a “global”  $k_0$ .

$\bar{\delta}(\beta)$  depends on the choice of the wave number  $k_0$  of the “basic” stripes. Analysis of striped patterns  $u_{st}(\mathbf{x}) = A \sin(\mathbf{k} \cdot \mathbf{x})$  and target patterns  $u_t(\mathbf{x}) = A \cos(kr)$  shows that  $\bar{\delta}(1)$  is minimized when  $k_0 = k = |\mathbf{k}|$ . Studies of textured patterns from model equations indicate (see Fig. 3) the presence of a unique minimum of  $\bar{\delta}(1)$ . We use the minimization of  $\bar{\delta}(1)$  as the criterion for the choice of the wave number  $k_0$  in Eq. (1). For patterns generated using the Swift-Hohenberg equation [6],  $k_0$  is very close to the wave number obtained by minimizing the “energy” [25]. We also find that our estimation of  $k_0$  is far more robust (i.e., smaller variation between distinct patterns) than that evaluated from the power spectrum. This is presumably because wavelength variations and curvature of contour lines at each location of the pattern contribute to the computation of  $\bar{\delta}(\beta)$ .

The variation in  $k$  over the pattern (traditionally defined to be the half-width of the structure factor [27]) can be estimated using the variation of  $\bar{\delta}(1)$  with the wave number  $k$  (see Fig. 3). In the remainder of the paper we define  $\Delta k$  to be the distance between  $k$  values for which  $\bar{\delta}(1)$  is twice the minimum value [26]. Analysis of textures shows that  $\Delta k$  is a configuration-independent, intensive variable.

Observe that our choice of  $k_0$  is arbitrary in one sense; we could have chosen to minimize  $\bar{\delta}(\beta)$  for any fixed  $\beta$  to determine  $k_0$ . However, the observed variations in  $k_0$  are insignificant. Alternatively, we could have evaluated *each*  $\bar{\delta}(\beta)$  by minimizing it with respect to  $k$ . We choose not to implement this scheme because of the need to estimate only

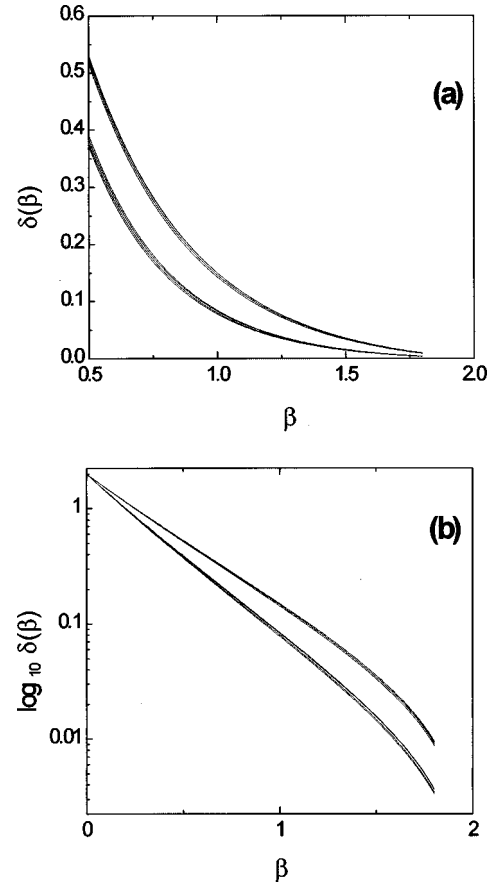


FIG. 4. The curves  $\bar{\delta}(\beta)$  for patterns generated at two different sets of control parameters. The lower bunch consists of curves for four patterns at the first set of control parameters (Fig. 1) while the upper bunch consists of those for a second set of control parameters (Fig. 2). (b) shows the same plots with a logarithmic vertical scale.

one free parameter (i.e., the wave number) for a given pattern.

For a perfect set of stripes the function  $\bar{\delta}(\beta) = 0$ . A domain wall contains curvature of the contour lines and variations of the stripe width; consequently it has nonzero disorder.  $\delta(\beta)$  for a single domain wall is a monotonically increasing function of the angle  $\theta$  between the stripes of the two domains [28]. Thus  $\delta(\beta)$  provides information absent in characterizations such as the correlation length.

The calculation of the disorder function from (typically noisy) grid values of the underlying field is described in Ref. [16]. It relies on a method to approximate a continuous function from values given on a grid referred to as the method of “distributed approximating functionals” (DAFs) [23].

### III. PATTERNS GENERATED USING THE SWIFT-HOHENBERG EQUATION

The patterns analyzed in the paper are obtained from periodic fields  $u(\mathbf{x}, t)$  generated by integrating random initial states through a modified Swift-Hohenberg equation (SHE) [29,6],

$$\partial_t u = D[\epsilon - (k_0^2 + \Delta)^2]u - \gamma u^3 - \nu(\nabla u)^2. \quad (2)$$

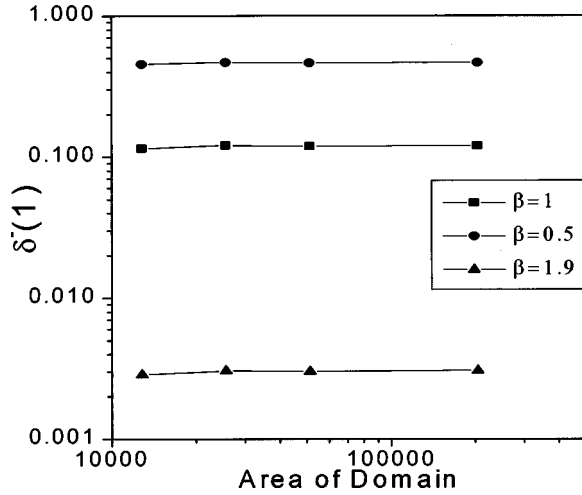


FIG. 5. The values of  $\bar{\delta}(0.5)$ ,  $\bar{\delta}(1.0)$ , and  $\bar{\delta}(1.9)$  for periodic patterns generated in domains of different sizes. The areas of the domains are  $36\pi \times 36\pi$ ,  $36\pi \times 72\pi$ ,  $72\pi \times 72\pi$ , and  $144\pi \times 144\pi$ . In each case random initial states are evolved for 8000 time units under the SHE with control parameter given in Fig. 2. The results indicate that  $\bar{\delta}(\beta)$  are intensive variables for labyrinthine patterns.

The parameters  $D$ ,  $k_0$ , and  $\gamma$  can be eliminated through suitable rescaling of  $t$ ,  $\mathbf{x}$ , and  $u$ , respectively.  $\epsilon$  measures the distance from the onset of patterns. The results for the variational case ( $\nu=0$ ) are presented in this section and those for the nonvariational case ( $\nu \neq 0$ ) are given in the next.

The initial fields for the integration were random numbers in a predetermined range. The time evolution is implemented using the alternating direction implicit algorithm [31]. Each nonlinear term  $N[u(\mathbf{x},t)]$  is expanded to first order in  $\delta u = u(\mathbf{x},t + \delta t) - u(\mathbf{x},t)$ , thus linearizing the equations in  $u(\mathbf{x},t + \delta t)$ . Updating the field involves the inversion of a pentadiagonal matrix. The typical time step used for the integration,  $\Delta t \sim 0.1$ , was chosen so that the higher-order terms in  $\delta u$  are insignificant. We have confirmed the robustness of the integration by comparing (in a few cases) the results with those done for a smaller time step ( $\Delta t \sim 0.001$ ).

### A. Properties of the disorder function

Analysis of patterns generated in model systems [16,30] and experimental systems [15] shows that the function  $\bar{\delta}(\beta)$  is configuration independent and differentiates patterns with different visual characteristics (see Fig. 4). The disorder function quantifies the characteristics of a labyrinthine pattern using the local curvature of the contour lines and the wavelength variations, which typically increase with the (visual) disorder of a texture. Thus,  $\bar{\delta}(\beta)$  is able to quantify (Fig. 4) the observation that patterns of Fig. 2 are more disordered than those of Fig. 1.

Next, we provide evidence to substantiate the claim that  $\bar{\delta}(\beta)$  are intensive variables for labyrinthine patterns such as those shown in Figs. 1 and 2 [32]. This is done by comparing values of  $\bar{\delta}(\beta)$  for patterns (with periodic boundary conditions) of several sizes. The sizes of the domains chosen are  $36\pi \times 36\pi$ ,  $36\pi \times 72\pi$ ,  $72\pi \times 72\pi$ , and  $144\pi \times 144\pi$ , and

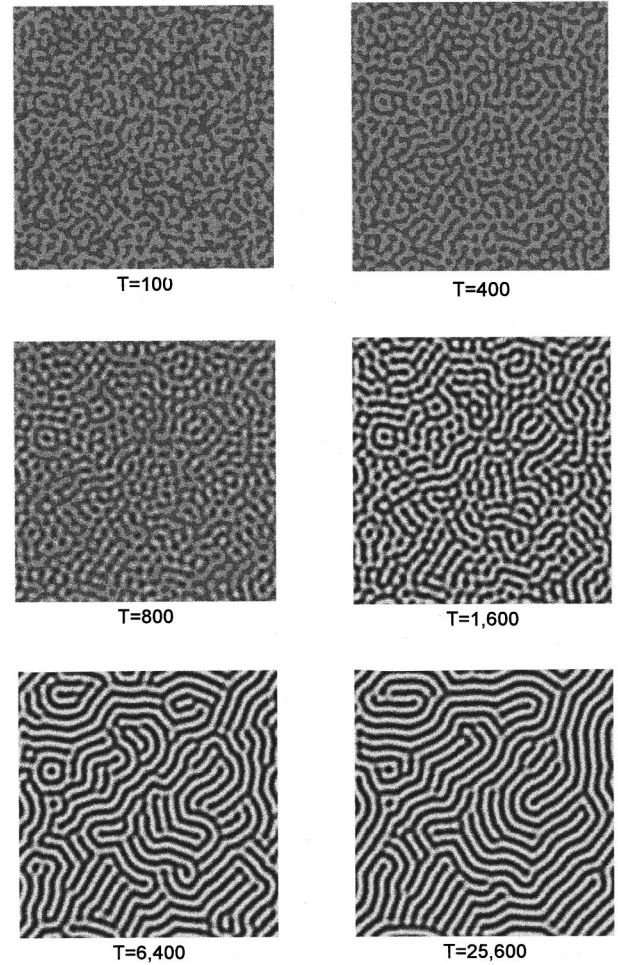


FIG. 6. Several snapshots [with time units defined in Eq. (2)] of the relaxation of a random initial state whose intensity is between  $\pm 10^{-2}$  under the SHE with  $D=0.01$ ,  $\epsilon=0.4$ ,  $\nu=0$ , and  $k_0=1/3$ . An initial phase ( $T < 800$ ) when the local striped patterns are being formed is followed by domain coarsening.

each pattern is generated by integrating a random initial state (with amplitude between  $\pm 10^{-2}$ ) for a time  $T=8000$  under the SHE. The results, shown in Fig. 5, give the mean of 10 patterns for each domain size (except the largest where only five patterns were used). The results indicate that  $\bar{\delta}(0.5)$ ,  $\bar{\delta}(1.0)$ , and  $\bar{\delta}(1.9)$  are intensive variables, and the corresponding  $\delta(\beta)$  are extensive variables.

### B. Relaxation of patterns

The characterization of textures using  $\bar{\delta}(\beta)$  finds one useful application in the study of the relaxation from an initially random state. Figure 6 shows several snapshots of a relaxing pattern. During an initial period ( $t < T_0 \sim 800$ ) the local domains emerge out of the random background and the mean intensity  $\langle |u(\mathbf{x},t)| \rangle$  nearly reaches its final value. The subsequent evolution due to domain coarsening is very slow. These qualitative features are repeated in multiple runs under the same control parameters.

Figure 7 shows the behavior of  $\Delta k$ ,  $\bar{\delta}(0.5)$ ,  $\bar{\delta}(1.0)$ , and  $\bar{\delta}(1.9)$  for the evolution shown in Fig. 6. The curves remain identical (except for small statistical fluctuations) for differ-

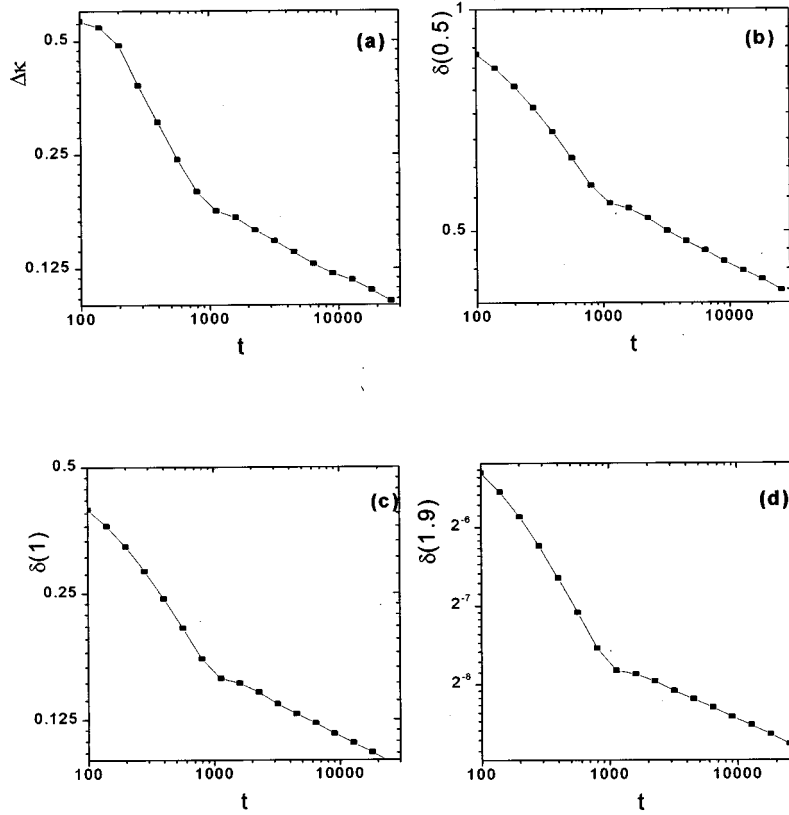


FIG. 7. The behavior of (a)  $\Delta k$ , (b)  $\bar{\delta}(0.5)$ , (c)  $\bar{\delta}(1)$ , and (d)  $\bar{\delta}(1.9)$  during the evolution shown in Fig. 6, with  $t$  given in units defined through Eq. (2). During the initial phase  $\bar{\delta}(\beta)$  decays (approximately) like  $t^{-(1/2)\beta}$ . During the second phase the scaling is nontrivial; e.g.,  $\bar{\delta}(0.5) \sim t^{-0.09}$ ,  $\bar{\delta}(1.0) \sim t^{-0.15}$ , and  $\bar{\delta}(1.9) \sim t^{-0.19}$ . The transition between the two phases occurs around  $t=800$ .

ent realizations of the experiment; i.e., the disorder function captures configuration-independent aspects of the organization of patterns. The relaxation clearly consists of two stages, with a sharp transition in  $\bar{\delta}(\beta)$  at  $t=T_0$  [10,12].

During the initial phase, the time evolution of  $\bar{\delta}(1)$  changes smoothly from a logarithmic decay to a power law  $\bar{\delta}(1) \sim t^{-\gamma_1}$ , where  $\gamma_1 \approx 0.5$ . Corresponding  $t^{-1/2}$  decay has been observed in the width of the structure factor [10]. The scaling is ‘‘trivial’’ in the sense that for other ‘‘moments’’  $\bar{\delta}(\beta) \sim t^{-(1/2)\beta}$  [33]. The decay of  $\bar{\delta}(\beta)$  is consistent with the  $L \sim t^{1/2}$  growth of domains in nonconserved systems [34].

The second phase of the relaxation (due to domain coarsening) exhibits a more complex behavior. The moments  $\bar{\delta}(0.5)$ ,  $\bar{\delta}(1)$ , and  $\bar{\delta}(1.9)$  behave approximately as  $t^{-0.09}$ ,  $t^{-0.15}$ , and  $t^{-0.20}$ , respectively, indicating the presence of ‘‘nontrivial’’ scaling [13]. The slower decay of  $\bar{\delta}(1.9)$  [compared to  $\bar{\delta}(1)^\beta$ ] suggests that changes in the density of defects are slower than the reduction of curvature of the contour lines [10].

### C. Changes in the relaxation with $\epsilon$

Figure 8 shows the behavior of  $\bar{\delta}(1)$  during the relaxation of random initial states under the SHE for several values of  $\epsilon$ , all other parameters being fixed. The initial decay of  $\bar{\delta}(1)$  and the rate of decay during the second phase are seen to be independent of  $\epsilon$ . Furthermore, the transition between the

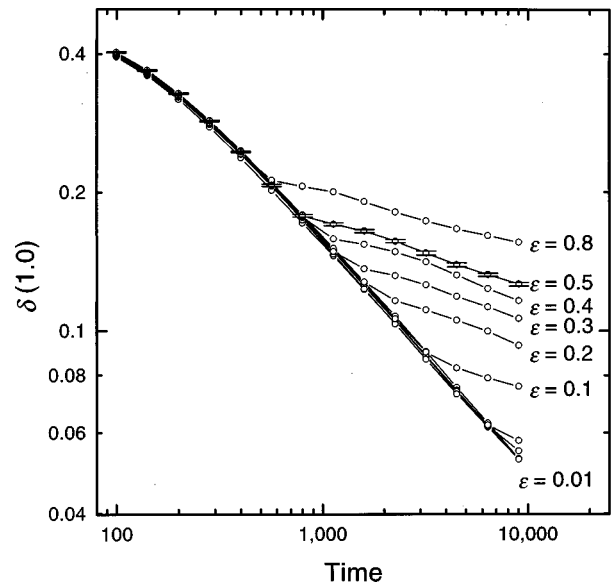


FIG. 8. The evolution of  $\bar{\delta}(1)$  for patterns generated by integrating random initial states under the SHE for several values of  $\epsilon$ . Each curve is an average of five runs, and time is measured in units described in Fig. 7. For clarity, the standard deviations are shown only for one parameter value. For distinct  $\epsilon$ ,  $\bar{\delta}(1)$  exhibits identical behavior during initial growth of domains, and decays at the same rate during the coarsening phase. The other moments  $\bar{\delta}(\beta)$  exhibit similar behavior.

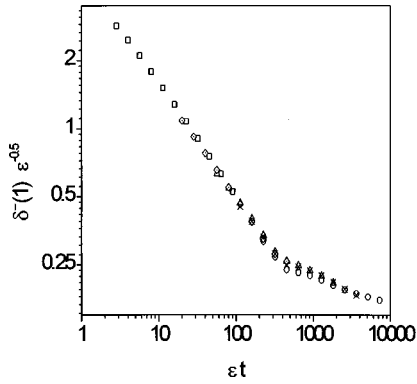


FIG. 9. The scaling function for the relaxation obtained by the rescaling  $t' = t\epsilon$  and  $\bar{\delta}' = \bar{\delta}\epsilon^{-1/2}$ . The data correspond to  $\epsilon$  values of 0.01, 0.05, 0.1, 0.4, and 0.8.

two phases advances with increasing  $\epsilon$ . Similar results are observed for all values of the moments  $\beta$ .

Suitable scaling of variables, including  $t \rightarrow \epsilon t$ , can be used to eliminate  $\epsilon$  from the SHE. Hence we expect that the rescaling  $t \rightarrow \epsilon t$  and  $\bar{\delta}(1) \rightarrow \epsilon^{-1/2} \bar{\delta}(1)$  will lead to collapse of the curves shown in Fig. 8. This is indeed the case as seen from the scaling function (Fig. 9).

#### IV. RELAXATION IN NONVARIATIONAL SYSTEMS

In this section we discuss properties of  $\bar{\delta}(\beta)$  when the spatio-temporal dynamics is nonvariational. The absence of an underlying “energy” of the dynamics suggests a faster relaxation, since the system cannot be constrained by “metastable states” during the evolution. The behavior of the disorder function confirms this expectation.

Figure 10 shows the behavior of  $\bar{\delta}(1)$  for the organization of a random field under a nonvariational SHE (i.e.,  $\nu \neq 0$ ). The decay of  $\bar{\delta}(1)$  remains the same (as the analogous variational dynamics) during the initial relaxation (Fig. 7) and becomes faster during the coarsening phase. As the coefficient  $\nu$  of the “nonvariational term” in Eq. (2) increases (the value of the remaining coefficients remaining the same), so

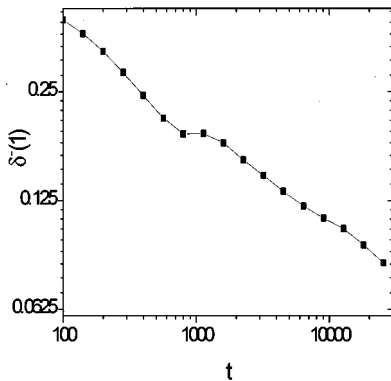


FIG. 10. The behavior of  $\bar{\delta}(1)$  for the evolution of a random initial state under the nonvariational modification of the SHE. The parameters of the SHE are the same as given in Fig. 6 except for  $\nu = 2.0$ . The initial decay is identical to the variational case while the coarsening phase exhibits a faster decay of  $\bar{\delta}(1)$ . The time  $t$  is measured in units described in Fig. 7.

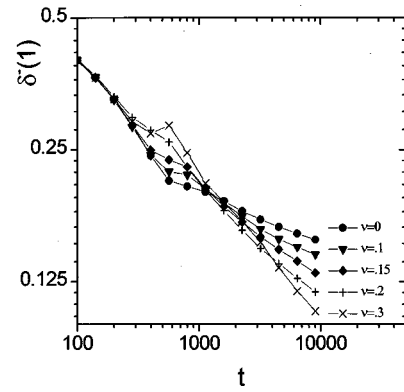


FIG. 11. The behavior of  $\bar{\delta}(1)$  for several values  $\nu$ . Observe that the decay during the growth phase remains the same, while the decay during the coarsening phase increases with  $\nu$ .

does the relaxation rate during the coarsening phase (Fig. 11).

The wave number [obtained by minimizing  $\bar{\delta}(1)$  over  $k_0$ ] relaxes to a value ( $k_0 = 0.61$ ) that is larger than the corresponding one for the variational case ( $k_0 = 0.59$ ). Such a deviation was observed earlier in Ref. [12], where it was suggested that  $k_0$  (for the nonvariational case) corresponds to the zero-climb velocity of isolated dislocation defects.

#### V. DISCUSSION

We have used the disorder function  $\bar{\delta}(\beta)$  to characterize properties of textured patterns and their relaxation from initially random states. The disorder function was defined by requiring its invariance under rigid motions of a single texture. It was found to be identical for multiple patterns generated under similar external conditions; i.e.,  $\bar{\delta}(\beta)$  is configuration independent. We provided evidence to confirm that the moments are intensive variables. In addition, the disorder function can differentiate between patterns with distinct characteristics.

The evolution of initially random states under the Swift-Hohenberg equation is conveniently described using  $\bar{\delta}(\beta)$ . The relaxation consists of two distinct stages separated by a sharp transition. During the initial phase, local striped domains emerge out of the noisy background and their amplitudes saturate close to their final value. This behavior is described by a logarithmic decay followed by a power-law decay of the disorder  $\bar{\delta}(1) \sim t^{-1/2}$ . The scaling is “trivial” in the sense that the decay of the remaining moments satisfies  $\bar{\delta}(\beta) \sim \bar{\delta}(1)^\beta$ . The second phase of the relaxation corresponds to domain coarsening and is a much slower process. The scaling during this phase is nontrivial.

As the system is driven further from the onset of patterns (as measured by the parameter  $\epsilon$ ), the duration of the initial phase is reduced. However, the rates of decay of the disorder function for the two phases remain unchanged and rescaling of time by  $\epsilon$  and of  $\bar{\delta}(\beta)$  by  $\epsilon^{-(1/2)\beta}$  leads to a scaling collapse.

The addition of nonvariational terms to the spatio-temporal dynamics leads to several interesting observations. The decay of disorder during the initial phase is unchanged,

and appears to be a model-independent feature. Thus, one may expect to observe it during relaxation of patterns in experimental systems. The expectation of a faster relaxation in nonvariational systems (due to the absence of ‘‘potential minima’’) is seen only during domain coarsening. This rate of relaxation is system dependent and increases as the coefficient of the nonvariational term.

There is very little theoretical understanding of the observed behavior of the disorder function. The decay of  $\bar{\delta}(\beta)$  during the initial phase of pattern relaxation is reminiscent of analogous behavior in the XY model [35,36], and appears to

correspond to the  $L \sim t^{1/2}$  growth of domains in nonconserved systems [34].

#### ACKNOWLEDGMENTS

We would like to thank K. Bassler, D. K. Hoffman, R. E. Jones, D. J. Kouri, and H. L. Swinney for many stimulating discussions. This work was partially funded by the U.S. Office of Naval Research and the Energy Laboratory at the University of Houston.

- 
- [1] Q. Ouyang and H. L. Swinney, *Nature (London)* **352**, 610 (1991).
- [2] M. S. Heutmaker and J. P. Gollub, *Phys. Rev. A* **35**, 242 (1987).
- [3] E. Bodenschatz, J. R. de Bruyn, G. Ahlers, and D. S. Cannel, *Phys. Rev. Lett.* **67**, 3078 (1991).
- [4] R. E. Rosensweig, *Ferrohydrodynamics* (Cambridge University Press, Cambridge, 1985).
- [5] F. Melo, P. Umbanhowar, and H. L. Swinney, *Phys. Rev. Lett.* **72**, 172 (1993).
- [6] M. C. Cross and P. C. Hohenberg, *Rev. Mod. Phys.* **65**, 851 (1993).
- [7] P. K. Jakobsen, J. V. Maloney, and A. C. Newell, *Phys. Rev. A* **45**, 8129 (1992).
- [8] M. Bestehorn, *Phys. Rev. E* **48**, 3622 (1993).
- [9] M. Golubitsky, I. Stewart, and D. G. Schaeffer, *Singularities and Groups in Bifurcation Theory* (Springer-Verlag, New York, 1988), Vol. 2.
- [10] K. R. Elder, J. Viñals, and M. Grant, *Phys. Rev. A* **46**, 7618 (1990).
- [11] Q. Ouyang and H. L. Swinney, *Chaos* **1**, 411 (1991).
- [12] M. C. Cross and D. I. Meiron, *Phys. Rev. Lett.* **75**, 2152 (1995).
- [13] J. J. Christensen and A. J. Bray, *Phys. Rev. E* **58**, 5364 (1998).
- [14] Q. Hou, S. Sasa, and N. Goldenfeld, *Physica A* **239**, 219 (1997).
- [15] G. H. Gunaratne, R. E. Jones, Q. Ouyang, and H. L. Swinney, *Phys. Rev. Lett.* **75**, 3281 (1995).
- [16] G. H. Gunaratne, D. K. Hoffman, and D. J. Kouri, *Phys. Rev. E* **57**, 5146 (1998).
- [17] A. Kudrolli, B. Pier, and J. P. Gollub, *Physica D* **123**, 99 (1998).
- [18] S. L. Judd and M. Silber (unpublished).
- [19] W. S. Edwards and S. Fauve, *Phys. Rev. E* **47**, R788 (1993).
- [20] D. Levine and P. J. Steinhardt, *Phys. Rev. Lett.* **53**, 2477 (1984).
- [21] L. Landau and E. Lifshitz, *Fluid Mechanics* (Pergamon Press, Oxford, 1959).
- [22] M. C. Cross, *Phys. Rev. A* **25**, 1065 (1982).
- [23] D. K. Hoffman, M. Arnold, and D. J. Kouri, *J. Phys. Chem.* **96**, 6539 (1992).
- [24] D. K. Hoffman, G. H. Gunaratne, D. Z. Zhang, and D. J. Kouri (unpublished).
- [25] Y. Pomeau and P. Manneville, *Phys. Lett.* **75A**, 296 (1980).
- [26] In general,  $\Delta k$  can be defined to be the distance between  $k$  values for which  $\bar{\delta}(1)$  is a factor  $F$  ( $>1$ ) of the minimum. Properties studied in the paper, such as the decay rates, are independent of  $F$ .
- [27] Y. Tu and M. C. Cross, *Phys. Rev. Lett.* **75**, 2152 (1995).
- [28] R. E. Jones, Ph. D. thesis, University of Houston (1997); R. E. Jones and G. H. Gunaratne, *J. Stat. Phys.* **93**, 427 (1998).
- [29] J. Swift and P. C. Hohenberg, *Phys. Rev. A* **15**, 319 (1977).
- [30] P. Gray and S. K. Scott, *Chem. Eng. Sci.* **38**, 29 (1983); *J. Phys. Chem.* **89**, 22 (1985).
- [31] W. H. Press, B. P. Flannery, S. A. Teukolsky, and W. T. Vetterling, *Numerical Recipes – The Art of Scientific Computing* (Cambridge University Press, Cambridge, 1988).
- [32] The disorder function is not intensive for patterns with global regularity, such as a single target pattern or a single domain wall.
- [33] The behavior during the entire first stage can be approximated by  $\bar{\delta}(\beta, t) = 1/(a + b \ln(t) + ct^{\beta/2})$ , for fixed  $a$ ,  $b$ , and  $c$ .
- [34] A. D. Rutenberg and A. J. Bray, *Phys. Rev. E* **51**, 5499 (1995).
- [35] K. Kawasaki, *Phys. Rev. A* **31**, 3880 (1985).
- [36] R. Loft and T. A. DeGrand, *Phys. Rev. B* **35**, 8528 (1987).